Published in final edited form as:

SIAM J Numer Anal. 2014 ; 52(4): 2027–2047. doi:10.1137/130919921.

TWO-GRID METHODS FOR MAXWELL EIGENVALUE PROBLEMS

J. ZHOU[†], **X. HU**[‡], **L. ZHONG**[§], **S. SHU**[†], and **L. CHEN**[¶]

J. ZHOU: xnuzj2004@163.com; X. HU: hu_x@math.psu.edu; L. ZHONG: zhong@scnu.edu.cn; S. SHU: shushi@xtu.edu.cn; L. CHEN: chenlong@math.uci.edu

[†]School of Mathematical and Computational Sciences, Xiangtan University, Xiangtan 411105, China

[‡]Department of Mathematics, Pennsylvania State University, University Park, PA 16802

[§]School of Mathematics Science, South China Normal University, Guangzhou 510631, China

[¶]Department of Mathematics, University of California at Irvine, Irvine, CA 92697

Abstract

Two new two-grid algorithms are proposed for solving the Maxwell eigenvalue problem. The new methods are based on the two-grid methodology recently proposed by Xu and Zhou [*Math. Comp.*, 70 (2001), pp. 17–25] and further developed by Hu and Cheng [*Math. Comp.*, 80 (2011), pp. 1287–1301] for elliptic eigenvalue problems. The new two-grid schemes reduce the solution of the Maxwell eigenvalue problem on a fine grid to one linear indefinite Maxwell equation on the same fine grid and an original eigenvalue problem on a much coarser grid. The new schemes, therefore, save total computational cost. The error estimates reveals that the two-grid methods maintain asymptotically optimal accuracy, and the numerical experiments presented confirm the theoretical results.

Keywords

two-grid method; Maxwell eigenvalue problem; edge element

1. Introduction

In this paper, we develop efficient algorithms for computing the Maxwell eigenvalue problem, which is a basic and important computational model in computational electromagnetism, e.g., in regard to electromagnetic waveguides and resonances in cavities (see, e.g., [7, 12, 33, 39]). The governing equations are

$$\operatorname{curl}(\mu_r^{-1}\operatorname{curl}\boldsymbol{u})=\omega^2\varepsilon_r\boldsymbol{u} \qquad \text{in } \Omega, \quad (1.1)$$

$$\operatorname{div}(\varepsilon_r\boldsymbol{u})=0 \qquad \text{in } \Omega, \quad (1.2)$$

$$\gamma_t \boldsymbol{u} = 0 \qquad \text{on } \partial\Omega, \quad (1.3)$$

where $\Omega \subset \mathbb{R}^n (n=2,3)$ is a bounded Lipschitz polyhedron domain and $\gamma_t \boldsymbol{u}$ is the tangential trace of $\boldsymbol{u}$. The coefficients μ_r and ε_r are the real relative magnetic permeability and electric permittivity, respectively, that satisfy the Lipschitz continuous condition, whereas ω is the resonant angular frequency of the electromagnetic wave for cavity Ω. In the following sections, we will use the conventional notation λ to replace ω^2.

Edge finite element methods for solving the Maxwell eigenvalue problem are widely used and their convergences have been studied extensively (see [8, 11, 20] and references therein). Imposing the divergence-free constraint in the discretization is a challenging task. The divergence-free constraint (1.2) can be dropped from the weak formulation and imposed implicitly. Though dropping the constraint may introduce spurious eigenvalues, doing so will not affect the nonzero eigenvalues (see, e.g., [20, 36, 31, 30, 48]). An alternative is the so-called mixed formation. In a mixed formulation, a Lagrange multiplier is introduced to impose the divergence-free constraint (1.2) in a weak sense. Using the mixed discretization, no spurious eigenvalue will be introduced. However, the resulting linear algebraic system is larger and of the saddle point type such that it is difficult to solve (see, e.g., [1, 2, 36]). Another approach is the penalty method which relies on explicitly imposing the divergence-free condition by introducing a penalty term (see, e.g., [9, 17, 31]). Compared with the discretized linear system that arises from the mixed method, the system from the penalty method is considerably smaller. However, the penalty method also introduces spurious eigenvalues.

For all the methods referring to Maxwell eigenvalue problems above, a large-scale discrete eigenvalue problem has to be solved, which is very challenging and time-consuming. Multigrid methods for computing eigenvalues of symmetric and positive definite cases, e.g., [5, 21, 28, 29, 38], are not applicable directly for the Maxwell eigenvalue problems due to the large kernel of the differential operator curl. To steer the inverse iterations away from the kernel of curl, Hiptmair and Neymeyr [30] proposed the so-called projected preconditioned inverse iteration method; see also [13] for the extension to adaptivity. In each inverse iteration, multigrid methods are applied in order to solve a shifted Maxwell equation and an additional Poisson equation with the purpose of imposing the weak divergence-free constraint. It takes 10 to 20 iterations to converge to an acceptable tolerance [30].

Here, we focus on speeding up the iterations by using a two-grid approach. The two-grid method, first introduced by Xu [43, 44], has been applied to many problems, such as nonlinear elliptic problems [45], nonlinear parabolic equations [18, 19], Navier–Stokes problems [25, 35], and Maxwell equations [50, 51]. In regard to the presented study, most relevant work is the two-grid method for elliptic eigenvalue problems developed by Xu and Zhou [46]. The main idea proposed by Xu and Zhou [46] is to reduce the solution of an eigenvalue problem on a given fine grid with mesh size h to the solution of the same eigenvalue problem on a much coarser grid with mesh size $H \gg h$, which can be easily solved as the size of the discrete eigenvalue problem is significantly smaller than the

original eigenvalue problem on the fine grid, and the solution of a linear problem on the same fine grid, which can be solved by mature and efficient numerical algorithms.

In this paper, we adopt this idea and develop efficient two-grid methods for solving the Maxwell eigenvalue problems. That is, we first solve a Maxwell eigenvalue problem on a coarse grid and then solve a linear Maxwell equation on a fine grid. Essentially, the procedure is similar to performing only one step of the Rayleigh quotient iteration using a good initial guess from the coarse grid. It provides a competitive approach for computing the Maxwell eigenvalue problems. Although generalizing the two-grid approach to the Maxwell eigenvalue problems seems straightforward, several nontrivial theoretical and practical issues must be addressed.

First, it is important to note that the standard two-grid method (Xu and Zhou [46]) for elliptic eigenvalue problems works when the order of error in the L^2 norm is one order higher than the error in the energy norm. Therefore, on the fine grid, a simple linear equation, which comes from the inverse iteration (or the fixed point iteration in general), can be used to maintain the asymptotically optimal accuracy for $H^2 = h$. In terms of approximation of the Maxwell equations, it is well-known that establishing an L^2 norm error estimate is a very challenging task [52]. For example, for the first family edge element, we cannot expect the error in the L^2 norm has higher convergence rate than the error in the energy norm. As a result, in order to make the two-grid algorithm work, on the fine grid, we must solve linear Maxwell equations derived from the shifted inverse iteration. This idea is proposed in [34, 47] as an acceleration scheme for the standard two-grid method of elliptic eigenvalue problems.

For the shifted inverse iteration, we need to solve an indefinite and nearly singular Maxwell equation on the fine grid. However, it is difficult to solve this equation such that very efficient solvers are required. Because we are interested in small eigenvalues, the wave number of this indefinite Maxwell problem is relatively small. We will use the preconditioned minimal residual (P-MINRES) including the shift Laplacian technique [23, 22] and the HX preconditioner [32] for the corresponding definite linear equation. Again since we are interested in the approximation of eigenvalues, we discard the standard relative residual norm but use the approximation of eigenvalues as the stopping tolerance of P-MINRES. Our numerical computation shows that the solver with the modified stopping tolerance converges in a few steps, which is almost uniform with respect to the size of the problem. In summary, we reduce solving the Maxwell eigenvalue problem to solving a Maxwell equation for which efficient solvers/preconditioners are available.

Another problem introduced by the shifted inverse iteration is the divergence-free constraint which only holds weakly on the coarse grid. It is possible to explicitly impose this constraint on the fine grid by projecting the obtained approximated eigenfunction on the coarse grid to the discrete divergence-free space on the fine grid by solving an extra Poisson equation. However, our analysis, which is based on the Helmholtz decomposition and an estimate of the differences between the weakly divergence-free functions on coarse and fine grids, shows that even without the projection step, our two-grid method produces an

approximation λ^h to λ and remains asymptotically convergence rate for $H^3 = h$. When the domain is smooth and convex, the rate of convergence is

$$|\lambda - \lambda^h| \leq C(H^6 + h^6).$$

Note that $H^3 = h$ implies that a very coarse mesh can be used—which saves considerably computational cost and time, especially in three dimensions. For example, for a three-dimensional unit cube, $h = 1/64$, the number of unknowns is 1, 872, 064, whereas for $H = h^{1/3} = 1/4$ there are only 604 unknowns.

On the other hand, we require the coarse grid to be fine enough to be able to capture the information we are interested in. This fact somehow limits us to choosing too-coarse grids in our two-grid algorithms, but it is a standard requirement for solving eigenvalue problems.

The rest of this paper is organized as follows. In section 2, we introduce the Maxwell eigenvalue problem. Section 3 presents new algorithms proposed in this paper, as well as some notes about the algorithms. In section 4, we show the error estimates of our two-grid methods for the Maxwell eigenvalue problem. And, in section 5, we give some numerical examples in two and three dimensions to demonstrate the efficiency of our new methods.

2. Preliminary

Denote by

$$\boldsymbol{H}_0(\mathrm{curl};\Omega) = \begin{cases} \{\boldsymbol{u} \in (L^2(\Omega))^2 : \mathrm{curl}\, \boldsymbol{u} \in L^2(\Omega), \gamma_t \boldsymbol{u} = 0\} & (\text{if } n=2) \\ \{\boldsymbol{u} \in (L^2(\Omega))^3 : \mathrm{curl}\, \boldsymbol{u} \in (L^2(\Omega))^3, \gamma_t \boldsymbol{u} = 0\} & (\text{if } n=3) \end{cases},$$

equipped with the norm $\|\boldsymbol{u}\|_{\mathrm{curl}} := \left(\|\boldsymbol{u}\|^2 + \|\mathrm{curl}\, \boldsymbol{u}\|^2\right)^{\frac{1}{2}}$ The tangential trace is $\gamma_t \boldsymbol{u} = \boldsymbol{u} \times \boldsymbol{n}$ in three dimensions, whereas the tangential trace is $\gamma_t \boldsymbol{u} = \boldsymbol{u}\, \boldsymbol{t}$ in two dimensions with $\boldsymbol{n}$ denoting the outer unit normal vector and $\boldsymbol{t}$ the unit tangential vector on boundary $\Gamma = \partial\Omega$. Define $X := \{\boldsymbol{u} \in \boldsymbol{H}_0(\mathrm{curl}; \Omega), \mathrm{div}(\varepsilon_r \boldsymbol{u}) = 0 \text{ in } \Omega\}$.

The variational form of the Maxwell eigenvalue problem (1.1)–(1.3) is as follows: find $(\lambda, \boldsymbol{u}) \in \mathbb{R}^+ \times X$ and $\boldsymbol{u} \neq 0$ satisfying

$$a(\boldsymbol{u}, \boldsymbol{v}) = \lambda\, b(\boldsymbol{u}, \boldsymbol{v}) \quad \text{for all } \boldsymbol{v} \in X, \quad (2.1)$$

where

$$a(\boldsymbol{u}, \boldsymbol{v}) = (\mu_r^{-1} \mathrm{curl}\boldsymbol{u}, \mathrm{curl}\boldsymbol{v}),$$
$$b(\boldsymbol{u}, \boldsymbol{v}) = (\varepsilon_r \boldsymbol{u}, \boldsymbol{v}).$$

We use $(\cdot,\cdot)$ for the standard L^2-inner product and define a weight L^2-inner product $(\cdot,\cdot)_B = b(\cdot,\cdot)$.

It is easy to check that the bilinear form $a(\boldsymbol{u}, \boldsymbol{v})$ satisfies the following conditions (see Corollary 4.4 in [31]):

$$a(\boldsymbol{u}, \boldsymbol{v}) \leq C_1 ||\boldsymbol{u}||_{\mathrm{curl}} ||\boldsymbol{v}||_{\mathrm{curl}} \text{ for all } \boldsymbol{u}, \boldsymbol{v} \in X,$$
$$a(\boldsymbol{u}, \boldsymbol{u}) \geq C_2 ||\boldsymbol{u}||^2_{\mathrm{curl}} \text{ for all } \boldsymbol{u} \in X.$$

Define an operator $A : X \to X' \approxeq X$ such that $\langle A_{\boldsymbol{u},\boldsymbol{v}} \rangle = a(\boldsymbol{u}, \boldsymbol{v})$; therefore, A is compact and self-adjoint on X. By virtue of the Hilbert–Schmidt theory (see [31, 40]), there exists an infinite discrete set of eigenvalues $\{\lambda_k\}$ and the corresponding eigenfunctions $\boldsymbol{u}_k \in X$, $k = 1, 2, 3, \ldots$, satisfy (2.1).

As the divergence-free constraint (1.2) is difficult to impose in the discretization, we will consider a modified variational problem: find $(\lambda, \boldsymbol{u}) \in \mathbb{R}^+ \times \boldsymbol{H}_0(\mathrm{curl};\Omega)$ and $\mathbf{u} \not\equiv 0$ satisfying

$$a(\boldsymbol{u}, \boldsymbol{v}) = \lambda b(\boldsymbol{u}, \boldsymbol{v}) \text{ for all } \boldsymbol{v} \in \boldsymbol{H}_0(\mathrm{curl};\Omega). \quad (2.2)$$

That is, we solve the eigenvalue problem in a space larger than X. The eigenfunction corresponding to $\lambda \neq 0$ remains unchanged [8]. Because for $\lambda \neq 0$, by taking $\boldsymbol{v} = \nabla p$ in (2.2), $p \in H_0^1(\Omega)$, we have

$$a(\boldsymbol{u}, \nabla p) = \lambda b(\boldsymbol{u}, \nabla p) = \lambda(\varepsilon_r \boldsymbol{u}, \nabla p) = 0 \text{ for all } p \in H_0^1(\Omega),$$

which implies a divergence-free constraint (1.2) in the weak sense. However, now zero is an eigenvalue of (2.2) and the corresponding eigenspace is the infinite dimensional space $\nabla H_0^1(\Omega)$ when the domain Ω is simple.

We will consider the finite element approximation based on the modified variational form (2.2). Let $\mathscr{T}_h$ be a conforming triangulation of the domain Ω. The lowest-order edge element defined on $\mathscr{T}_h$ is

$$\boldsymbol{V}_h = \left\{ \mathbf{u}_h \in \boldsymbol{H}_0(\mathrm{curl};\Omega) \middle| \mathbf{u}_h|_\tau = \boldsymbol{a}_\tau + \boldsymbol{b}_\tau \times \boldsymbol{x} \text{ for all } \tau \in \mathscr{T}_h \right\}, \quad (2.3)$$

and the discrete divergence-free space is

$$X_h = \left\{ \mathbf{u}_h \in \boldsymbol{V}_h \middle| b(\mathbf{u}_h, \nabla q) = 0 \text{ for all } q \in S_h^0 \right\}, \quad (2.4)$$

where S_h^0 is the standard linear Lagrangian finite element space with zero trace such that $\nabla S_h^0 \subset \boldsymbol{V}_h$.

The finite element discretization of (2.2) is as follows: find $(\lambda_h, \boldsymbol{u}_h) \in \mathbb{R} \times \boldsymbol{V}_h$ and $\boldsymbol{u}_h \not\equiv 0$ satisfying

$$a(\boldsymbol{u}_h, \boldsymbol{v}_h) = \lambda_h b(\boldsymbol{u}_h, \boldsymbol{v}_h) \text{ for all } \boldsymbol{v}_h \in \boldsymbol{V}_h. \quad (2.5)$$

Based on the same argument, for $\lambda_h \neq 0$, the corresponding finite element approximation $\boldsymbol{u}_h$ implicitly satisfies the discrete divergence-free constraint, i.e., $\boldsymbol{u}_h \in X_h$. Therefore, nonzero eigenvalues λ_h and the corresponding eigenfuctions $\boldsymbol{u}_h$ satisfy

$$a(\boldsymbol{u}_h, \boldsymbol{v}_h) = \lambda_h b(\boldsymbol{u}_h, \boldsymbol{v}_h) \text{ for all } \boldsymbol{v}_h \in X_h. \quad (2.6)$$

We use $(\boldsymbol{u}_i, \lambda_i)$ to denote the continuous eigen-pairs and $(\boldsymbol{u}_{h,i}, \lambda_{h,i})$ to denote the discrete eigen-pairs and order them as follows:

$$\lambda_1 \leq \lambda_2 \leq \cdots \leq \lambda_i \leq \cdots,$$
$$\lambda_{h,1} \leq \lambda_{h,2} \leq \cdots \leq \lambda_{h,i} \leq \cdots.$$

The following error estimate, which can be found in [8, Theorem 5.4], is useful in our analysis.

Theorem 2.1

Let λ_i be an eigenvalue of problem (2.1) with multiplicity m_i, and denote by $M(\lambda_i)$ the corresponding eigenspace. Then, exactly m_i eigenvalues of problems (2.6) $\lambda_{h,i_1}, \ldots, \lambda_{h,i_{m_i}}$ converge to λ_i. By denoting $M_h(\lambda_i)$ as the direct sum of the eigenspaces corresponding to $\lambda_{h,i_1}, \ldots, \lambda_{h,i_{m_i}}$, we have that there exists h_0 such that for $0 < h < h_0$, the following inequalities hold:

$$\begin{aligned} |\lambda_i - \lambda_{h,i_j}| &\leq C(\rho_1(h)+\rho_2(h))^2 \quad for\ all\ j=1,\ldots,m_i, \\ \sigma(M(\lambda_i), M_h(\lambda_i)) &\leq C(\rho_1(h)+\rho_2(h)), \end{aligned} \quad (2.7)$$

where C is a constant independent of h and $\sigma(M(\lambda_i), M_h(\lambda_i))$ denote the gap between $M(\lambda_i)$ and $M(\lambda_i)$, which is defined as

$$\sigma(M(\lambda_i), M_h(\lambda_i)) = max(\overline{\sigma}(M(\lambda_i), M_h(\lambda_i)), \overline{\sigma}(M_h(\lambda_i), M(\lambda_i))),$$
$$\overline{\sigma}(M(\lambda_i), M_h(\lambda_i)) = \sup_{\boldsymbol{u}_i \in M(\lambda_i)} \inf_{\boldsymbol{u}_{i,h} \in M_h(\lambda_i)} ||\boldsymbol{u}_i - \boldsymbol{u}_{i,h}||_{\text{curl}}.$$

Remark 2.1

Due to the space restriction, we refer to [8] for the definitions of ρ_1, ρ_2. Here we only list examples of ρ_1, ρ_2 related to our work. When Ω is a Lipschitz polyhedron, $X \subset (H^{1/2+\delta}(\Omega))^3$ [26, 6, 40], and consequently $\rho_1(h) = \rho_2(h) = \mathcal{O}(h^{1/2+\delta})$ for some $0 < \delta \leq \frac{1}{2}$. And, when Ω is smooth or convex, $\delta = 1/2$ and $\rho_1(h) = \rho_2(h) = \mathcal{O}(h)$. The details can be found in [8].

At the end of this section, we give an important identity that relates the error in the eigenvalue to the eigenfunction approximation. The proof is standard and can be found, for example, in Lemma 3.1 of [4].

Proposition 2.2

Let $(\lambda, \mathbf{u})$ be an eigen-pair of (2.1) or (2.2) with $\lambda \neq 0$. For any $\boldsymbol{w} \in \boldsymbol{H}_0(\text{curl}; \Omega) \backslash \{0\}$, we have

$$\frac{a(\boldsymbol{w},\boldsymbol{w})}{b(\boldsymbol{w},\boldsymbol{w})}-\lambda=\frac{a(\boldsymbol{w}-\boldsymbol{u},\boldsymbol{w}-\boldsymbol{u})}{b(\boldsymbol{w},\boldsymbol{w})}-\lambda\frac{b(\boldsymbol{w}-\boldsymbol{u},\boldsymbol{w}-\boldsymbol{u})}{b(\boldsymbol{w},\boldsymbol{w})}.$$

3. Two-grid methods

In this section, we present our two-grid methods for the Maxwell eigenvalue problems. We will prove the error estimates in the next section.

3.1. Main algorithms

Let $\mathscr{T}_H$ and $\mathscr{T}_h$ each be triangulations of the domain Ω with different mesh size H and h, where $H > h$. Usually, $\mathscr{T}_h$ is a refinement of $\mathscr{T}_H$. The finite element spaces associated with $\mathscr{T}_H$ and $\mathscr{T}_h$ are denoted by $\boldsymbol{V}_H$ and $\boldsymbol{V}_h$, respectively. Based on these two grids, we present the following two-grid methods for Maxwell eigenvalue problems.

Algorithm 1.

1 Solve a Maxwell eigenvalue problem on the coarse grid $\mathscr{T}_H$ find $(\lambda_H, \boldsymbol{u}_H) \in \mathbb{R}^+ \times \boldsymbol{V}_H$ and $\boldsymbol{u}_H \neq 0$ satisfying

$$a(u_H, v_H) = \lambda_H b(u_H, v_H) \text{ for all } v_H \in V_H. \quad (3.1)$$

2 Solve a Poisson equation on the fine grid: find $p_h \in S_h$ such that

$$(\varepsilon_r \nabla p_h, \nabla q_h) = b(u_H, \nabla q_h) \text{ for all } q_h \in S_h^0. \quad (3.2)$$

Then update $\boldsymbol{u}_H^h \in X_h$ by $\boldsymbol{u}_H^h = \boldsymbol{u}_H - \nabla p_h$.

3 Solve an indefinite Maxwell equation on the fine grid $\mathscr{T}_h$: find $\boldsymbol{u}^h \in \boldsymbol{V}_h$ such that

$$a(u^h, v_h) - \lambda_H b(u^h, v_h) = b(u_H^h, v_h) \text{ for all } v_h \in V_h. \quad (3.3)$$

4 Use the Rayleigh quotient to compute the approximate eigenvalue on the fine grid:

$$\lambda^h = \frac{a(u^h, u^h)}{b(u^h, u^h)}. \quad (3.4)$$

Algorithm 2.

1 Solve a Maxwell eigenvalue problem on the coarse grid $\mathscr{T}_H$: find $(\lambda_H, \boldsymbol{u}_H) \in \mathbb{R}^+ \times \boldsymbol{V}_H$ and $\boldsymbol{u}_H \neq 0$ satisfying

$$a(u_H, v_H) = \lambda_H b(u_H, v_H) \text{ for all } v_H \in V_H. \quad (3.5)$$

2 Solve an indefinite Maxwell equation on the fine grid $\mathscr{T}_h$: find $\boldsymbol{u}^h \in \boldsymbol{V}_h$ such that

$$a(u^h, v_h) - \lambda_H b(u^h, v_h) = b(u_H, v_h) \text{ for all } v_h \in V_h. \quad (3.6)$$

3 Use the Rayleigh quotient to compute the approximate eigenvalue on the fine grid:

$$\lambda^h = \frac{a(u^h, u^h)}{b(u^h, u^h)}. \quad (3.7)$$

We present two algorithms here. They differ in regard to the ways in which they handle the divergence-free condition. In Algorithm 1, we project $\boldsymbol{u}_H$ to X_h by solving one Poisson equation. However, in Algorithm 2, we skip this step. Our error estimates in the next section prove that both algorithms are effective. Algorithm 2 is cheaper in terms of computational cost and, consequently, more efficient. Therefore, we recommend using it in preference to Algorithm 1. On the coarse grid, we solve a Maxwell eigenvalue problem based on the variational form (2.5). As the coarse grid problem is small, any robust method can be used in this step. We assume that solving the Maxwell eigenvalue problem on the coarse grid is inexpensive and that the total computational work is negligible compared with the work associated to the linear system on the fine grid.

Remark 3.1—Algorithms 1 and 2 can be naturally used to compute multiple eigenvalues as long as the coarse grid is fine enough. Assume that an eigenvalue λ has multiplicity q and its corresponding eigenfunctions are $\boldsymbol{u}^1, \boldsymbol{u}^2, \ldots, \boldsymbol{u}^q$. In our two-grid algorithms, we first need to compute q approximated eigenfunctions $\boldsymbol{u}_H^1, \boldsymbol{u}_H^2, \ldots, \boldsymbol{u}_H^q$, on the coarse grid. Then we use each $\boldsymbol{u}_H^m, m=1, 2, \ldots, q$, to proceed with the two-grid algorithms. For example, in Algorithm 2, we use $\boldsymbol{u}_H^m, m=1, 2, \ldots, q$, in (3.6) to compute $\boldsymbol{u}^{h,m}$, $m = 1, 2, \ldots, q$. Finally, we compute the Rayleigh quotient of $\boldsymbol{u}^{h,m}$, $m = 1, 2, \ldots, q$, to get q approximate eigenvalues $\lambda^{h,m}$, $m = 1, 2, \ldots, q$, on the fine level. These eigenvalues are approximations of the eigenvalue λ with multiplicity q and the space spanned by $\boldsymbol{u}^{h,m}$, $m = 1, 2, \ldots, q$, is an approximation of the eigenspace spanned by $\boldsymbol{u}^m$, $m = 1, 2, \ldots, q$, of the eigenvalue λ. Note that the computed eigenfunctions $\boldsymbol{u}^{h,m}$, $m = 1, 2, \ldots, q$, may not be orthogonal, but an orthogonal basis of the space spanned by $\boldsymbol{u}^{h,m}$, $m = 1, 2, \ldots., q$, can be easily obtained by an orthogonalization procedure, for example, the Gram–Schmidt algorithm.

Remark 3.2—Similar to the multiple eigenvalues case discussed in Remark 3.1, Algorithms 1 and 2 can be naturally used to compute clustered eigenvalues as long as the coarse grid is fine enough. For the sake of simplicity, assume two eigenvalues λ_1 and λ_2 are close but not equal to each other. We require that the coarse level is fine enough to capture the gap between two different eigenvalues, i.e., we should be able to get two approximations $\lambda_{H,1}$ and $\lambda_{H,2}$, which approximate λ_1 and λ_2, respectively. Then we can proceed with the two-grid algorithms as discussed in Remark 3.1 and get two approximate eigen-pairs $\left(\lambda_1^h, \boldsymbol{u}_1^h\right)$ and $\left(\lambda_2^h, \boldsymbol{u}_2^h\right)$ on the fine level. The error estimate we presented later will be amplified by the factor $1/|\lambda_1 - \lambda_2|$.

On the fine grid, it is necessary to solve an indefinite Maxwell equation, which is based on the idea of using the approximation on the coarse grid as an initial guess in the Newton's iteration. As we shall explain next, this is different from the classical two-grid method for eigenvalue problems.

Consider the abstract eigenvalue problem $\mathscr{A}u=\lambda u$ with a compact operator $\mathscr{A}$. If we use the approximation on the coarse grid u_H and λ_H as an initial guess, and apply one step of the fixed-point iteration, we obtain $\mathscr{A}u^h=\lambda_H u_H$. Roughly speaking, this describes the two-grid method proposed by Xu and Zhou [46]. Due to the linear convergence rate of the fixed-point iteration, if

$$||u-u_H||+|\lambda-\lambda_H|=\mathscr{O}\left(H^2\right), \quad (3.8)$$

then we can expect the resulting two-grid method has asymptotical convergence rate $\mathscr{O}(h)+\mathscr{O}(H^2)$. However, for the first family edge element, an optimal L^2 error estimate such as (3.8) is not available as the polynomial space is incomplete. Consequently, two-grid methods based on the fixed-point iteration may not work.

The two-grid algorithms we propose are based on the generalization of the accelerated two-grid scheme proposed by Hu and Cheng [34], which can also be viewed as a variant of the Newton's method for the eigenvalue problems. Let us reformulate the eigenvalue problem as the following nonlinear problem:

$$F(u_h,\lambda_h):=\mathscr{A}_h u_h-\lambda_h u_h=0.$$

By applying the Newton's method with u_H and λ_H from the coarse grid as the initial guess, we have

$$\nabla F(u_H,\lambda_H)\begin{pmatrix}\delta u\\ \delta\lambda\end{pmatrix}=-F(u_H,\lambda_H)$$

and more specifically

$$(\mathscr{A}_h-\lambda_H I-u_H)\begin{pmatrix}\delta u\\ \delta\lambda\end{pmatrix}=-(\mathscr{A}_h u_H-\lambda_H u_H),$$

which can be reformulated as

$$(\mathscr{A}_h-\lambda_H I)(u_H+\delta u)=\delta\lambda u_H. \quad (3.9)$$

We cannot solve one equation (3.9) for two unknowns δu and $\delta\lambda$. However, a crucial observation is that $\delta\lambda$ on the right-hand side can be treated as a scaling which will not affect the Rayleigh quotient of the eigenfunction. More precisely, consider the problem without the scaling $\delta\lambda$ on the right-hand side:

$$(\mathscr{A}_h-\lambda_H I)u^h=u_H. \quad (3.10)$$

It is, therefore, easy to show that $\delta\lambda\, u^h = \tilde{u}^h := u_H + \delta u$. Moreover, an important fact is that

$$\lambda^h=\frac{(\mathscr{A}_h u^h, u^h)}{(u^h, u^h)}=\frac{(\mathscr{A}_h \tilde{u}^h, \tilde{u}^h)}{(\tilde{u}^h, \tilde{u}^h)}.$$

This means that solving the problem (3.10) could lead to the same approximation of the eigenvalue as can be achieved with the Newton's iteration, which suggests the second step in our two-grid algorithms.

3.2. Efficiency and solver

Our main reason for proposing the two-grid methods is to address the high computational cost of solving a large-size eigenvalue problem. Among the existing methods for the Maxwell eigenvalue problem, the standard inverse iteration is one of the most popular methods, although it is difficult to find a good initial vector and it is necessary to solve a large positive semidefinite Maxwell equation. Furthermore, the solution must be projected onto the orthogonal complements of the kernels in every iteration.

A two-grid scheme can reduce the discrete eigenvalue problem on a fine grid $\mathscr{T}_h$ to the same problem on a much coarser grid $\mathscr{T}_H$ and only *one* shifted inverse iteration on the fine grid $\mathscr{T}_h$. The accuracy of $\mathscr{O}(h^2+H^6)$ (assume the domain is smooth and convex) as shown in the next section allows us to use a very coarse grid, which makes the computational cost on the coarse grid negligible. Therefore, the dominate cost of the two-grid methods is solving an indefinite and nearly singular Maxwell problem on the fine grid.

For the coarse grid eigenvalue problem (3.5), it is a generalized algebraic eigenvalue problem which is small in size. We can solve the problem directly, for example, using the eigs function in MATLAB. For (3.6) on the fine grid, we need to solve an indefinite Maxwell equation. As we are usually interested in several small eigenvalues, we combine the shift Laplacian technique [15, 22] with the HX preconditioner [32] in order to design an efficient solver.

Write (3.6) in the following matrix form:

$$(\mathbb{A}_h - \lambda_H \mathbb{M}_h)\mathrm{u}^h=\mathrm{b}. \quad (3.11)$$

In this notation, $\mathbb{A}_h=(a(\phi_j,\phi_i))_{ij}$ is the stiffness matrix, $\mathbb{M}_h=(b(\phi_j,\phi_i))_{ij}$ is the mass matrix, and b is the load vector. This is a symmetric indefinite system. We choose the MINRES method with the shifted Laplacian preconditioner $(\mathbb{A}_h+\lambda_H \mathbb{M}_h)^{-1}$, which is further approximated by the well-known HX preconditioner [32]. In our numerical experiments, one step of the HX preconditioner is used in every MINRES iteration and the numerical results show that such a solver is effective and robust.

For the stopping criterion of the MINRES method, we choose the accuracy of $\varepsilon=|\lambda_h^i-\lambda_h^{i+1}|/\lambda_h^{i+1}$, where *i* means the iteration step, rather than the standard relative residual $||\mathrm{b}-(\mathbb{A}_h-\lambda_H\mathbb{M}_h)\mathrm{u}^{h,i}||/||b||$. We made this choice for the following two reasons: (1) the final goal is to solve an eigenvalue problem and approximate the eigenvalues, and (2)

the iteration error is almost entirely within the space spanned by the eigenvectors (see, e.g., [34]), such that the error will not affect the Rayleigh quotient. An alternative stopping criterion is $\varepsilon = \|r^{i+1} - r^i\| / \|r^i\|$, where $r^i = A_h u^{h,i} - \lambda_h^i M_h u^{h,i}$. Note that in the definition of r^i, λ_h^i instead of λ_H is used since the eigen-pair we are computing is $(\lambda_h^i, u^{h,i})$. We can also use the stopping criterion $\varepsilon = \min\left\{|\lambda_h^i - \lambda_h^{i+1}|/\lambda_h^{i+1}, \|r^{i+1} - r^i\|/\|r^i\|\right\}$ which includes both eigenvalues and eigenfunctions. These choice of accuracy reduces the number of iteration steps dramatically comparing with the standard choice of the relative residual.

Remark 3.3—When λ_H is close to the close eigenvalue λ_h on the fine level, the indefinite problems on the fine level in our two-grid algorithms become nearly singular and seem to be more challenging to solve. This problem has been much discussed in the literature in the context of general inverse power method. As shown in, e.g., [27, 42, 41], the near-singularity of this system hardly presents a problem due to the fact that, for eigenvalue problem, the near null space of this system is exactly spanned by the eigenfunctions that we are interested in. A detailed discussion can be found, for example, in Remark 3.2 in [34].

4. Error estimate

In this section, we will give an error estimate of both our two-grid methods, Algorithms 1 and 2, for the Maxwell eigenvalue problems.

4.1. Error estimate of Algorithm 1

Assuming that the eigenvalue λ has multiplicity q, let

$$M(\lambda) = \{\boldsymbol{u} \in X : \boldsymbol{u} \text{ is an eigenvect or of } (2.1) \text{ corresponding to } \lambda\}$$

be the eigenspace corresponding to the eigenvalue λ. Let $\Lambda = \{\lambda_{h,i}, i = 1, \ldots, q\}$ be approximated eigenvalues of eigenvalue λ by solving the variational problem (2.5). Let $\boldsymbol{u}_{h,i}$ denote the eigenvectors corresponding to $\lambda_{h,i}$ for $i = 1, \ldots, q$. Similarly, let

$$M_h(\lambda) = \text{span}\{\boldsymbol{u}_{h,1}, \boldsymbol{u}_{h,2}, \ldots, \boldsymbol{u}_{h,q}\}$$

be the approximate eigenspace corresponding to the eigenvalue λ.

Given a positive constant μ, define the following bilinear form:

$$a_\mu^+(\boldsymbol{u}, \boldsymbol{v}) = a(\boldsymbol{u}, \boldsymbol{v}) + \mu b(\boldsymbol{u}, \boldsymbol{v}) \quad \text{for all } \boldsymbol{u}, \boldsymbol{v} \in X. \quad (4.1)$$

It is well-known that (see Lemma 4.10 in [40])

$$|a_\mu^+(\boldsymbol{u}, \boldsymbol{v})| \le C\|\boldsymbol{u}\|_{\text{curl}}\|v\|_{\text{curl}} \quad \text{for all } \boldsymbol{u}, \boldsymbol{v} \in X,$$
$$|a_\mu^+(\boldsymbol{u}, \boldsymbol{v})| \ge C\|\boldsymbol{u}\|_{\text{curl}}^2 \quad \text{for all } \boldsymbol{u} \in X,$$

where the constant C depends on μ_r, ε_r, and μ but is independent of $\boldsymbol{u}$ and $\boldsymbol{v}$. A similar statement is also true for space X_h, i.e.,

$$|a_\mu^+(\boldsymbol{u}_h, \boldsymbol{v}_h)| \le C\|\boldsymbol{u}_h\|_{\mathrm{curl}}\|\boldsymbol{v}_h\|_{\mathrm{curl}} \ \text{ for all } \boldsymbol{u}_h, \boldsymbol{v}_h \in X_h,$$
$$|a_\mu^+(\boldsymbol{u}_h, \boldsymbol{v}_h)| \ge C\|\boldsymbol{u}_h\|_{\mathrm{curl}}^2 \ \text{ for all } \boldsymbol{u}_h \in X_h,$$

where the constant C also depends on μ_r, ε_r, and μ but is independent of $\boldsymbol{u}_h$, $\boldsymbol{v}_h$, and the mesh size h. Moreover, we can define the operators K: $(L^2(\Omega))^n \to (L^2(\Omega))^n$ and K_h: $(L^2(\Omega))^n \to (L^2(\Omega))^n$ such that

$$a_\mu^+(K\ f, \boldsymbol{v}) = -2\mu b(f, \boldsymbol{v}) \ \text{ for all } \boldsymbol{v} \in X, \quad (4.2)$$

$$a_\mu^+(K_h\ f, \boldsymbol{v}_h) = -2\mu b(f, \boldsymbol{v}_h) \ \text{ for all } \boldsymbol{v}_h \in X_h. \quad (4.3)$$

The following lemma has been shown in [40].

Lemma 4.1 (Theorem 4.11 in [40])—The operators K and K_h are bounded and compact from $L^2(\Omega)$ into $L^2(\Omega)$. In addition,

$$\|K\ f\|_{\mathrm{curl}} \le C\|f\|_{L^2}, \quad (4.4)$$

$$\|K_h\ f\|_{\mathrm{curl}} \le C\|f\|_{L^2}, \quad (4.5)$$

where the constants C only depend on μ_r, ε_r, and μ.

Both K and K_h are compact and their eigenvalues are $-2\mu/(\lambda+\mu)$ and $-2\mu/(\lambda_h+\mu)$, respectively, where λ and λ_h are eigenvalues of the Maxwell eigenvalue problem (2.1) and (2.6). Therefore, we have the following estimate for the operator $(I+K_h)^{-1}$ restricted to the orthogonal complement of $M_h(\lambda)$ in X_h, which will play an important role in the error analysis for our two-grid methods.

Lemma 4.2—Let $M_h^\perp(\lambda)$ denote the orthogonal complement of $M_h(\lambda)$ in X_h with respect to $b(\cdot,\cdot)$. Then we have

$$\|(I+K_h)^{-1}\|_{M_h^\perp(\lambda)\to M_h^\perp(\lambda)} = \left(\min_{\lambda_{h,j}\notin\Lambda}\left|\frac{\lambda_{h,j}-\mu}{\lambda_{h,j}+\mu}\right|\right)^{-1}. \quad (4.6)$$

Let $\rho = \min_{\lambda_j\neq\lambda}|\lambda_j - \lambda$. Assume that h is small enough such that $|\lambda_{h,j} - \lambda_j| \le \frac{1}{4}\rho$ for $\lambda_j \neq \lambda$ and assume that $|\mu - \lambda| \le \frac{1}{4}\rho$. Then we have

$$\min_{\lambda_{h,j}\notin\Lambda}\left|\frac{\lambda_{h,j}-\mu}{\lambda_{h,j}+\mu}\right| \geq \frac{\rho}{4\lambda+2\rho}=:C_{\rho,\lambda}^{-1}>0.$$

Proof: The identity (4.6) directly follows from the fact that

$$(I+K_h)^{-1}:M_h^{\perp}(\lambda)\to M_h^{\perp}(\lambda).$$

and the operator $(I + K_h)^{-1}$ is self-adjoint with respect to the inner product $b(\cdot,\cdot)$.

Note that $|\lambda_{h,j}-\mu| \geq \|\lambda_j-\lambda|-|\mu-\lambda|-|\lambda_j-\lambda_{h,j}\| \geq \frac{1}{2}\rho$; then we have $0<\lambda_{h,j}\leq \mu-\frac{1}{2}\rho \geq \|$ or $\lambda_{h,j}\geq \mu+\frac{1}{2}\rho$. Therefore,

$$\min_{\lambda_{h,j}\notin\Lambda}\left|\frac{\lambda_{h,j}-\mu}{\lambda_{h,j}+\mu}\right| \geq \min_{0<x\leq\mu-\frac{1}{2}\rho \text{ or } x\geq\mu+\frac{1}{2}\rho}\left|\frac{x-\mu}{x+\mu}\right|=\frac{\rho}{4\mu+\rho} \geq \frac{\rho}{4\lambda+2\rho}>0. \quad (4.7)$$

□

The following lemma shows that the discrete divergence-free function can be approximated by a continuous divergence-free function. Such a construction for the case $\varepsilon_r = 1$ is used, for example, in Girault [24] and [3], and a detailed proof can be found in [31, 40].

Lemma 4.3 (Lemma 4.5 in [31])—Let $\boldsymbol{u}_h \in X_h$ and Ω be a bounded Lipschitz polyhedron. There exists a $\boldsymbol{u} \in \boldsymbol{H}0$ (curl; Ω) satisfying

$$\mathrm{curl}\boldsymbol{u}=\mathrm{curl}\boldsymbol{u}_h,\ \ \mathrm{div}(\varepsilon_r\boldsymbol{u})=0,\ \ in\,\Omega, \quad (4.8)$$

and

$$\|\boldsymbol{u}-\boldsymbol{u}_h\|_0 \leq Ch^{1/2+\delta}\|\mathrm{curl}\boldsymbol{u}_h\|_0, \quad (4.9)$$

where the constants C and $0 < \delta \leq 1/2$ are independent of h, $\boldsymbol{u}$, and $\boldsymbol{u}_h$.

The following lemma, which can be found in [3], provides an error estimate for the solution of the Poisson problem (3.2) on the fine grid in the two-grid algorithm.

Lemma 4.4 (Proposition 4.4 in [3])—Under the assumptions of Lemma 4.3, let p_h, $\boldsymbol{u}_H^h$, $\boldsymbol{u}_H$ be defined as in Algorithm 1. Then we have

$$\|\nabla p_h\|_{L^2}=\|\boldsymbol{u}_H-\boldsymbol{u}_H^h\|_{L2} \leq CH^{1/2+\delta}\|\mathrm{curl}\,\boldsymbol{u}_H\|_{L^2}, \quad (4.10)$$

where the constant C and $0 < \delta \leq 1/2$ are independent of h and $\boldsymbol{u}_H$.

Proof: Note that $\boldsymbol{u}_H^h=\boldsymbol{u}_H-\nabla p_h$,

$$b(\boldsymbol{u}_H^h, \nabla q_h) = b(\boldsymbol{u}_H - \nabla p_h, \nabla q_h) = 0 \ \text{ for all } q_h \in S_h^0,$$

which implies $\boldsymbol{u}_H^h$ is discrete divergence-free in S_h^0. Then, by Lemma 4.3, there exists a $\boldsymbol{w} \in \boldsymbol{H}_0(\text{curl}; \Omega)$ satisfying

$$\text{curl}\boldsymbol{w} = \text{curl}\, \boldsymbol{u}_H^h, \ \ \text{div}(\varepsilon_r \boldsymbol{w}) = 0, \quad (4.11)$$

$$\|\boldsymbol{w} - \boldsymbol{u}_H^h\|_0 \le Ch^{1/2+\delta} \|\text{curl}\boldsymbol{u}_H^h\|_0. \quad (4.12)$$

Furthermore, (3.1) implies that $\boldsymbol{u}_H$ is discrete divergence-free in S_H^0. Based on Lemma 4.3 again, there exists a $\tilde{\boldsymbol{w}} \in \boldsymbol{H}_0(\text{curl}; \Omega)$ that satisfies

$$\text{curl}\tilde{\boldsymbol{w}} = \text{curl}\boldsymbol{u}_H, \ \text{div}(\varepsilon_r \tilde{\boldsymbol{w}}) = 0, \quad (4.13)$$

$$\|\tilde{\boldsymbol{w}} - \boldsymbol{u}_H\|_0 \le CH^{1/2+\delta} \|\text{curl}\boldsymbol{u}_H\|_0. \quad (4.14)$$

In view of (4.11) and (4.13), we know that

$$\boldsymbol{w} - \tilde{\boldsymbol{w}} \in X, \ \text{and curl}(\boldsymbol{w} - \tilde{\boldsymbol{w}}) = \text{curl}(\boldsymbol{u}_H^h - \boldsymbol{u}_H) = \text{curl}(-\nabla p_h) = 0,$$

which implies $\boldsymbol{w} - \tilde{\boldsymbol{w}}$.

Finally, as $\boldsymbol{u}_H^h = \boldsymbol{u}_H - \nabla p_h$ and $\boldsymbol{w} - \tilde{\boldsymbol{w}}$, by the inequalities (4.12) and (4.14),

$$\|\nabla p_h\|_{L^2} = \|\boldsymbol{u}_H - \boldsymbol{u}_H^h\|_{L^2} \le \|\boldsymbol{u}_H - \tilde{\boldsymbol{w}}\|_{L^2} + \|\boldsymbol{w} - \boldsymbol{u}_H^h\|_{L^2} \le CH^{1/2+\delta} \|\text{curl}\boldsymbol{u}_H\|_0.$$

This completes the proof. □

Now we are ready to provide an error estimate of Algorithm 1.

Theorem 4.5—Let λ_H and $(\lambda^h, \boldsymbol{u}^h)$ be computed by Algorithm 1 and λ_H is an approximation of the eigenvalue λ. Under the assumptions of Lemmas 4.2 and 4.4, there exists an eigenfunction $\boldsymbol{u} \in M(\lambda)$ such that

$$\min_{\alpha \in \mathbb{R}} \|\boldsymbol{u} - \alpha \boldsymbol{u}^h\|_{L^2} \le C(h^{1/2+\delta} + H^{3(1/2+\delta)}), \quad (4.15)$$

$$\min_{\alpha \in \mathbb{R}} \|\boldsymbol{u} - \alpha \boldsymbol{u}^h\|_{\text{curl}} \le C(h^{1/2+\delta} + H^{3(1/2+\delta)}). \quad (4.16)$$

And for the eigenvalue, we have

$$|\lambda - \lambda^h| \leq C(h^{1+2\delta} + H^{3(1+2\delta)}). \quad (4.17)$$

where the constants C depend only on μ_r, ε_r, ρ, λ, and $\boldsymbol{u}$, and $\delta \in (0, 1/2]$ depends only on the domain.

Proof: Let us define the operator A_h: $X_h \to X_h$ as

$$(A_h \boldsymbol{u}, \boldsymbol{v})_B = a(\boldsymbol{u}, \boldsymbol{v}) \text{ for all } \boldsymbol{u}, \boldsymbol{v} \in X_h.$$

Suppose eigenvalue λ is a multiple eigenvalue with multiplicity q. Let the eigen-pair ($\lambda_{h,i}$, $\boldsymbol{u}_{h,i}$), for some $i \in \{1, \ldots, q\}$, be one approximation of (λ, $\boldsymbol{u}$) by solving (2.5) which satisfies the relation (2.6)

$$A_h \boldsymbol{u}_{h,i} = \lambda_{h,i} \boldsymbol{u}_{h,i} \text{ in } X_h. \quad (4.18)$$

If $\lambda_H = \lambda_{h,j}$ for some $j \in \{1, \ldots, q\}$. Then the estimate is obtained by Theorem 2.1. We thus assume $\lambda_H \neq \lambda_{h,j}$ for all $j \in \{1, \ldots, q\}$. Since λ_H approximates λ, we also assume the coarse grid size H is fine enough such that λ_H is not equal to eigenvalues of A_h other than $\lambda_{h,j}$. Therefore $A_h - \lambda_H I$ is invertible. Let $\tilde{\boldsymbol{u}}^h \in X_h$ be the solution of the operator equation:

$$(A_h - \lambda_H I)\tilde{\boldsymbol{u}}^h = (\lambda_{h,i} - \lambda_H)\boldsymbol{u}_H^h \text{ in } (X_h, (\cdot,\cdot)_B). \quad (4.19)$$

Here $(X_h, (\cdot,\cdot)_B)$ means the Hilbert space X_h endowed with inner product $(\cdot,\cdot)_B$.

From (4.18) and (4.19), we have the error equation

$$(A_h - \lambda_H I)(\boldsymbol{u}_{h,i} - \tilde{\boldsymbol{u}}^h) = (\lambda_{h,i} - \lambda_H)(\boldsymbol{u}_{h,i} - \boldsymbol{u}_H^h) \text{ in } (X_h, (\cdot,\cdot)_B). \quad (4.20)$$

We decompose $\boldsymbol{u}_{h,i} - \boldsymbol{u}_H^h$ on the right-hand side as

$$\boldsymbol{u}_{h,i} - \boldsymbol{u}_H^h = (\boldsymbol{u}_{h,i} - E_h \boldsymbol{u}_H^h) + (E_h \boldsymbol{u}_H^h - \boldsymbol{u}_H^h).$$

where E_h is the orthogonal projection of X_h, w.r.t. to $(\cdot,\cdot)_B$, onto $M_h(\lambda)$. We can thus rewrite the error equation (4.20) as

$$(A_h - \lambda_H I)(\hat{\boldsymbol{u}}_{h,i} - \tilde{\boldsymbol{u}}^h) = (\lambda_{h,i} - \lambda_H)(E_h \boldsymbol{u}_H^h - \boldsymbol{u}_H^h), \quad (4.21)$$

where $\hat{\boldsymbol{u}}_{h,i} = \boldsymbol{u}_{h,i} - (\lambda_{h,i} - \lambda_H)(A_h - \lambda_H I)^{-1}(\boldsymbol{u}_{h,i} - E_h \boldsymbol{u}_H^h)$.

Now it is crucial to observe that $A_h - \lambda_H I$: $M_h(\lambda) \to M_h(\lambda)$ and $A_h - \lambda_H I : M_h^{\perp}(\lambda) \to M_h^{\perp}(\lambda)$ are an isomorphism since $M_h(\lambda)$ is an eigenspace of operator and λ_H is not an eigenvalue of A_h.

Then since $\boldsymbol{u}_{h,i} - E_h\boldsymbol{u}_H^h \in M_h(\lambda)$ and $\boldsymbol{u}_{h,i} \in M_h(\lambda)$, we conclude $\hat{\boldsymbol{u}}_{h,i} \in M_h(\lambda)$. Similarly $(E_h\boldsymbol{u}_H^h - \boldsymbol{u}_H^h) \in M_h^{\perp}(\lambda)$ implies $(\hat{\boldsymbol{u}}_{h,i} - \tilde{\boldsymbol{u}}^h) \in M_h^{\perp}(\lambda)$.

Following an argument similar to that in [40], we can define a vector $\mathscr{F}_{h,i} \in X_h$ such that

$$(A_h+\lambda_H I)\mathscr{F}_{h,i}=(\lambda_{h,i} - \lambda_H)(E_h\boldsymbol{u}_H^h - \boldsymbol{u}_H^h) \text{ in } X_h.$$

Therefore, we have $\mathscr{F}_{h,i} \in M_h^{\perp}(\lambda_i)$ and

$$\|\mathscr{F}_{h,i}\|_{\mathrm{curl}} \le C|\lambda_{h,i} - \lambda_H|\|E_h\boldsymbol{u}_H^h - \boldsymbol{u}_H^h\|_{L^2}.$$

By the definition of K_h with $\mu = \lambda_H$, problem (4.21) is equivalent to

$$(I+K_h)(\hat{\boldsymbol{u}}_{h,i} - \tilde{\boldsymbol{u}}^h)=\mathscr{F}_{h,i}.$$

Therefore, we have

$$\begin{aligned}\|\hat{\boldsymbol{u}}_{h,i} - \tilde{\boldsymbol{u}}^h\|_{L^2} &\le \|(I+K_h)^{-1}\|_{M_h^{\perp}(\lambda)\to M_h^{\perp}(\lambda)}\|\mathscr{F}_h\|_{L^2}\\ &\le C_\rho\|\mathscr{F}_{h,i}\|_{L^2}\\ &\le C_\rho C|\lambda_{h,i} - \lambda_H|\|E_h\boldsymbol{u}_H^h - \boldsymbol{u}_H^h\|_{L^2}.\end{aligned}$$

According to to the standard error estimate of $\boldsymbol{u}_H$ (see [8, 31]), there exists $\overline{\boldsymbol{u}}_h \in M_0(\lambda)$ such that $\|\overline{\boldsymbol{u}}_h - \boldsymbol{u}_H\|_{L^2} \le CH^{1/2+\delta}$. Therefore, we have

$$\|E_h\boldsymbol{u}_H^h - \boldsymbol{u}_H^h\|_{L^2} \le \|\overline{\boldsymbol{u}}_h - \boldsymbol{u}_H^h\|_{L^2} \le \|\overline{\boldsymbol{u}}_h - \boldsymbol{u}_H\|_{L^2}+\|\boldsymbol{u}_H - \boldsymbol{u}_H^h\|_{L^2} \le CH^{1/2+\delta},$$

where we use Lemma 4.4 in the last inequality. Then due to the standard estimate $|\lambda_{h,i} - \lambda_H| \le|\lambda - \lambda_{h,i}| + |\lambda - \lambda_H| \le CH^{1+2\delta}$, we have

$$\|\hat{\boldsymbol{u}}_{h,i} - \tilde{\boldsymbol{u}}^h\|_{L^2} \le CH^{3/2+3\delta}. \quad (4.22)$$

In view of the above procedure, we also have

$$\|\mathscr{F}_{h,i}\|_{\mathrm{curl}} \le C|\lambda_{h,i} - \lambda_H|\|E_h\boldsymbol{u}_H^h - \boldsymbol{u}_H^h\|_{L^2} \le CH^{3/2+3\delta}. \quad (4.23)$$

On the other hand, $(\hat{\boldsymbol{u}}_{h,i} - \tilde{\boldsymbol{u}}^h)=\mathscr{F}_{h,i} - K_{h,i}(\hat{\boldsymbol{u}}_{h,i} - \tilde{\boldsymbol{u}}^h)$ such that

$$\|\mathrm{curl}(\hat{\boldsymbol{u}}_{h,i} - \tilde{\boldsymbol{u}}^h)\|_{L^2} \le \|\hat{\boldsymbol{u}}_{h,i} - \tilde{\boldsymbol{u}}^h\|_{\mathrm{curl}} \le C(\|\mathscr{F}_{h,i}\|_{\mathrm{curl}}+\|(\hat{\boldsymbol{u}}_{h,i} - \tilde{\boldsymbol{u}}^h)\|_{L^2}) \le CH^{3/2+3\delta}.$$

where (4.23), Lemma 4.1, and inequality (4.22) are used.

Moreover, since $\sigma(M(\lambda), M_h(\lambda)) \leq Ch^{1/2+\delta}$, there exists $\boldsymbol{u} \in M(\lambda)$ such that $\|\boldsymbol{u} - \hat{\boldsymbol{u}}_{h,i}\|_{\mathrm{curl}} \leq Ch^{1/2+\delta}$ and consequently

$$\|\boldsymbol{u} - \tilde{\boldsymbol{u}}^h\|_{L^2} \leq \|\boldsymbol{u} - \hat{\boldsymbol{u}}_{h,i}\|_{L^2} + \|\hat{\boldsymbol{u}}_{h,i} - \tilde{\boldsymbol{u}}^h\|_{L^2} \leq C(h^{1/2+\delta} + H^{3/2+3\delta}). \quad (4.24)$$

$$\|\boldsymbol{u} - \tilde{\boldsymbol{u}}^h\|_{\mathrm{curl}} \leq \|\boldsymbol{u} - \hat{\boldsymbol{u}}_{h,i}\|_{\mathrm{curl}} + \|\hat{\boldsymbol{u}}_{h,i} - \tilde{\boldsymbol{u}}^h\|_{\mathrm{curl}} \leq C(h^{1/2+\delta} + H^{3/2+3\delta}). \quad (4.25)$$

Note that $\tilde{\boldsymbol{u}}^h = (\lambda_{h,i} - \lambda_H)\boldsymbol{u}^h$. Then the estimates (4.15) and (4.16) follow directly.

Using the triangle inequality and $\|\boldsymbol{u}\|_{L^2} = 1$, we have

$$\|\tilde{\boldsymbol{u}}^h\|_{L^2} \geq \|\boldsymbol{u}\|_{L^2} - \|\boldsymbol{u} - \tilde{\boldsymbol{u}}^h\|_{L^2} \geq 1 - CH^{3/2+3\delta}. \quad (4.26)$$

Hence, we obtain a lower bound of $\|\tilde{\boldsymbol{u}}^h\|_{L^2}$ under the assumption H is small enough.

To get the estimate of the eigenvalue, by Proposition 2.2, the boundedness of μ_r and ε_r, (4.26), and the boundedness of λ, we have

$$\begin{aligned} |\lambda^h - \lambda| &= \left| \frac{a(\tilde{\boldsymbol{u}}^h - \boldsymbol{u}, \tilde{\boldsymbol{u}}^h - \boldsymbol{u})}{b(\tilde{\boldsymbol{u}}^h, \tilde{\boldsymbol{u}}^h)} - \lambda \frac{b(\tilde{\boldsymbol{u}}^h - \boldsymbol{u}, \tilde{\boldsymbol{u}}^h - \boldsymbol{u})}{b(\tilde{\boldsymbol{u}}^h, \tilde{\boldsymbol{u}}^h)} \right| \\ &\leq C \left(\|\mathrm{curl}(\boldsymbol{u} - \tilde{\boldsymbol{u}}^h)\|_{L^2}^2 + \lambda \|\boldsymbol{u} - \tilde{\boldsymbol{u}}^h\|_{L^2}^2 \right) \\ &\leq C(h^{1+2\delta} + H^{3+6\delta}), \end{aligned}$$

which gives the error estimate for the eigenvalue (4.17). □

Remark 4.1—For the case in which domain Ω is smooth or convex, we have $\delta = 1/2$ and

$$\min_{\alpha \in \mathbb{R}} \|\boldsymbol{u} - \alpha \boldsymbol{u}^h\|_{L^2} + \min_{\alpha \in \mathbb{R}} \|\boldsymbol{u} - \alpha \boldsymbol{u}^h\|_{\mathrm{curl}} \leq C(h + H^3),$$
$$|\lambda - \lambda^h| \leq C(h^2 + H^6).$$

4.2. Error estimate of Algorithm 2

Working in the divergence-free space X_h requires solving an extra Poisson problem on the fine grid. In this section, we discuss the convergence of Algorithm 2 based on the standard edge element spaces $\boldsymbol{V}_H$ and $\boldsymbol{V}_h$ and our analysis proves that this extra step can be skipped. Note that $\boldsymbol{V}_H \subset \boldsymbol{V}_h$.

In order to analyze Algorithm 2, again, we introduce the following auxiliary problem on the fine grid:

$$a(\breve{\boldsymbol{u}}^h, \boldsymbol{v}_h) - \lambda_H b(\breve{\boldsymbol{u}}^h, \boldsymbol{v}_h) = (\lambda_{h,i} - \lambda_H) b(\boldsymbol{u}_H, \boldsymbol{v}_h) \text{ for all } \boldsymbol{v}_h \in \boldsymbol{V}_h.$$

And we recall that the eigen-pair $(\lambda_{h,i}, \boldsymbol{u}_{h,i}) + \in \mathbb{R}^+ \times \boldsymbol{X}_h$ satisfies

$$a(\boldsymbol{u}_{h,i},\boldsymbol{v}_h)=\lambda_{h,i}b(\boldsymbol{u}_{h,i},\boldsymbol{v}_h)\ \text{ for all } \boldsymbol{v}_h\in\boldsymbol{V}_h$$

and thus obtain the following equation, which is similar to (4.20) but imposed on $\boldsymbol{V}_h$ instead of $\boldsymbol{X}_h$:

$$a(\boldsymbol{u}_{h,i}-\overset{\smile}{\boldsymbol{u}}^h,\boldsymbol{v}_h)-\lambda_H b(\boldsymbol{u}_{h,i}-\overset{\smile}{\boldsymbol{u}}^h,\boldsymbol{v}_h)=(\lambda_{h,i}-\lambda_H)b(\boldsymbol{u}_{h,i}-\boldsymbol{u}_H,\boldsymbol{v}_h),\ \ \boldsymbol{v}_h\in\boldsymbol{V}_h. \quad (4.27)$$

Note that $\boldsymbol{u}_{h,i}-\overset{\smile}{\boldsymbol{u}}^h=\boldsymbol{e}_{h,i}+\nabla\tilde{p}_h$ for some $\boldsymbol{e}_{h,i}\in X_h$ and $\tilde{p}_h\in S_h^0$, where $\tilde{p}_h$ can be determined by solving

$$-\lambda_H(\varepsilon_r\nabla\tilde{p}_h,\nabla q_h)=(\lambda_{h,i}-\lambda_H)b(\boldsymbol{u}_{h,i}-\boldsymbol{u}_H,\nabla q_h,)\ \text{ for all } q_h\in S_h^0. \quad (4.28)$$

Following [40], we can easily estimate $\tilde{p}_h$ as following.

Lemma 4.6

Under the assumptions of Lemma 4.4, we have

$$\|\nabla\tilde{p}_h\|_{L^2}=\frac{|\lambda_{h,i}-\lambda_H|}{\lambda_H}\|\nabla p_h\|_{L^2}\le CH^{3/2+3\delta}, \quad (4.29)$$

where p_h is defined by (3.2) and the constant C and $\delta\in(0,1/2]$ are independent of H.

Proof—Using (4.28), $\boldsymbol{u}_{h,i}\in X_h$, and (3.2), we have

$$\lambda_H(\varepsilon_r\nabla\tilde{p}_h,\nabla q_h)=(\lambda_{h,i}-\lambda_H)b(\boldsymbol{u}_H,\nabla q_h)=(\lambda_{h,i}-\lambda_H)(\varepsilon_r\nabla p_h,\nabla q_h)\text{for all } q_h\in S_h^0.$$

Then the result follows from Lemma 4.4 directly. □

Theorem 4.7

Let λ_H and $(\lambda^h,\boldsymbol{u}^h)$ be computed by Algorithm 2, and λ_H is an approximation of the eigenvalue λ. Under the assumptions of Lemmas 4.2 and 4.4 there then exists an eigenfunction $\boldsymbol{u}\in M(\lambda)$ such that

$$\min_{\alpha\in\mathbb{R}}\|\boldsymbol{u}-\alpha\boldsymbol{u}^h\|_{L^2}\le C(h^{1/2+\delta}+H^{3(1/2+\delta)}), \quad (4.30)$$

$$\min_{\alpha\in\mathbb{R}}\|\boldsymbol{u}-\alpha\boldsymbol{u}^h\|_{\mathrm{curl}}\le C(h^{1/2+\delta}+H^{3(1/2+\delta)}). \quad (4.31)$$

And for the eigenvalue, we have

$$|\lambda-\lambda^h|\le C(h^{1+2\delta}+H^{3(1+2\delta)}), \quad (4.32)$$

where the constant C and $0<\delta\le 1/2$ depend only on μ_r, ε_r, ρ, λ_i, and $\boldsymbol{u}$.

Proof—Substituting $\boldsymbol{u}_{h,i} - \breve{\boldsymbol{u}}^h = \boldsymbol{e}_{h,i} + \nabla\tilde{p}_h$ into (4.27), and using $\boldsymbol{u}_H^h = \boldsymbol{u}_H - \nabla p_h$, then for any $\boldsymbol{v}_h \in X_h$ we have

$$a(\boldsymbol{e}_{h,i}, \boldsymbol{v}_h) - \lambda_H b(\boldsymbol{e}_{h,i}, \boldsymbol{v}_h) = (\lambda_{h,i} - \lambda_H) b(\boldsymbol{u}_{h,i} - \boldsymbol{u}_H, \boldsymbol{v}_h) = (\lambda_{h,i} - \lambda_H) b(\boldsymbol{u}_{h,i} - \boldsymbol{u}_H^h, \boldsymbol{v}_h).$$

where we use $b(\nabla\tilde{p}_h, \boldsymbol{v}_h) = 0$ in the first identity and $b(\nabla p_h, \boldsymbol{v}_h) = 0$ in the second identity, for all $\boldsymbol{v}_h \in X_h$. Now, we can rewrite the above identity in the operator equation:

$$(A_h - \lambda_H I)\boldsymbol{e}_{h,i} = (\lambda_{h,i} - \lambda_H)(\boldsymbol{u}_{h,i} - \boldsymbol{u}_H^h) \text{ in } X_h \quad (4.33)$$

Comparing (4.33) with (4.20), we have $\boldsymbol{e}_{h,i} = \boldsymbol{u}_{h,i} - \tilde{\boldsymbol{u}}^h$, where $\tilde{\boldsymbol{u}}^h$ is defined in (4.19). Hence, we have $\breve{\boldsymbol{u}}^h = \tilde{\boldsymbol{u}}^h - \nabla\tilde{p}_h$.

Therefore, based on (4.24) and (4.25), there exists a $\boldsymbol{u} \in M(\lambda)$ such that

$$\|\boldsymbol{u} - \breve{\boldsymbol{u}}^h\|_{L^2} \le \|\boldsymbol{u} - \tilde{\boldsymbol{u}}^h\|_{L^2} + \|\nabla\tilde{p}_h\|_{L^2} \le C(h^{1/2+\delta} + H^{3(1/2+\delta)}) \quad (4.34)$$

and similarly

$$\|\boldsymbol{u} - \breve{\boldsymbol{u}}^h\|_{\mathrm{curl}} \le \|\boldsymbol{u} - \tilde{\boldsymbol{u}}^h\|_{\mathrm{curl}} + \|\nabla\tilde{p}_h\|_{L^2} \le C(h^{1/2+\delta} + H^{3(1/2+\delta)}). \quad (4.35)$$

This leads to (4.30) and (4.31). For the eigenvalue, using the triangle inequality and $\|\boldsymbol{u}\|_{L^2} = 1$, we have

$$\|\breve{\boldsymbol{u}}^h\|_{L^2} \ge \|\boldsymbol{u}\|_{L^2} - \|\boldsymbol{u} - \breve{\boldsymbol{u}}^h\|_{L^2} \ge 1 - CH^{3/2+3\delta}. \quad (4.36)$$

Equation (4.32) follows from Proposition 2.2. □

Remark 4.2

When Ω is smooth or convex, we have $\delta = 1/2$ and

$$\min_{\alpha\in\mathbb{R}} \|\boldsymbol{u} - \alpha\boldsymbol{u}^h\|_{L^2} + \min_{\alpha\in\mathbb{R}} \|\boldsymbol{u} - \alpha\boldsymbol{u}^h\|_{\mathrm{curl}} \le C(h + H^3),$$
$$|\lambda - \lambda^h| \le C(h^2 + H^6).$$

5. Numerical experiments

In this section, we will report several numerical experiments in two and three dimensions to verify the effectiveness and robustness of Algorithm 2. We implemented these experiments using the *i*FEM package [16]. We did the computation in double decision but only display six digits after the decimal in tables, which are accurate enough for quantity bigger than 10^{-6}.

Example 5.1

Consider the Maxwell eigenvalue problem (1.1)–(1.3) on the two-dimensional domain $\Omega = (0, 1) \times (0, 1)$ and $\mu_r = \varepsilon_r = 1$ in Ω. It is easy to show that $\lambda_1 = \lambda_2 = \pi^2$ and $\lambda_3 = 2\pi^2$.

The results shown in Tables 1–3 verify the theoretical expectations. Let $\lambda_{k,H}$ and $\lambda_{k,h}$ denote the eigenvalues computed by solving the eigenvalue problem (3.5) on the coarse grid $\mathscr{T}_H$ and the refined grid $\mathscr{T}_h$, respectively, and let λ_k^h denote the eigenvalue obtained by Algorithm 2, here $k = 1, 2, 3$. The coarse mesh $\mathscr{T}_H$ is the uniform triangular mesh. The fine grid $\mathscr{T}_h$ is obtained by applying several uniform refinements (every triangle is divided into four congruent triangles) from $\mathscr{T}_H$.

We design several tests to verify our error estimate. First, we fix a coarse mesh and vary the fine mesh. The mesh sizes satisfy the relation $h^2 \geq H^6$, and thus $\mathscr{O}(H^6)$ is smaller than $\mathscr{O}(h^2)$. From Table 1, it is evident that the approximation rate is indeed $\mathscr{O}(h^2)$. Second, we fix a fine mesh and vary the coarse mesh subject to the constraint $h^2 \geq H^6$. Table 2 shows that we can obtain the same level of accuracy by using different coarse meshes. In Table 2, a dash means that the computer we use does not have enough memory to solve the eigenvalue problem with direct solvers when the mesh size is too small. Third, in Table 3, we vary both the coarse and the fine meshes at the same time, subjected to $h^2 = H^6$, i.e., $\mathscr{O}(h^2+H^6)=\mathscr{O}(H^6)$. Similarly, we only need pay attention to whether the numerical results satisfy $|\lambda - \lambda^h|=\mathscr{O}(H^6)$. In fact, it is easy to find that the convergence rate is $\mathscr{O}(H^6)$, as shown in Table 3.

To sum up, we have used three different approaches to show that the numerical results are consistent with our theory. Tables 1–3 verify that $|\lambda - \lambda^h|=\mathscr{O}(h^2+H^6)$. Further, the solver introduced before is efficient. The most time-consuming part of the solver is the HX preconditioner. Therefore, we report the number of calls of the HX preconditioner. We compare our method with the inverse iteration method for computing eigenvalues. For the first eigenvalue, at each inverse iteration step, PCG using the HX preconditioner typically needs five or six iterations and typically 10 steps of inverse iteration are needed. For other eigenvalues, a shifted indefinite and near singular Maxwell equation should also be solved, and again around 10 steps of inverse iteration are needed to converge. Our method behaves essentially like one inverse iteration and thus reduces the total computational cost. We choose HX preconditioner as the computational cost unit because other measurements, such as CPU time, depends on the programming language, computational environment, and many other facts.

Example 5.2

Consider the Maxwell eigenvalue problem on a two-dimensional L-shaped domain $\Omega = (-1, 1)^2/(0, 1) \times (-1, 0)$ and $\mu_r = \varepsilon_r = 1$. $\lambda_1 = 1.47562182$ (see [10]).

We consider an L-shaped domain problem. The solution has a singularity at the origin and $\delta \neq 1/2$ in the analysis. We use a simple adaptive method for the twogrid method. The coarse grid $\mathscr{T}_0$ used in this numerical experiment is an adaptively refined grid. $\mathscr{T}_i$ is obtained by

uniform refinement (every triangle is divided into four) of $\mathcal{T}_{i-1}$ for $i = 1, 2, 3$; see Figure 1. From Table 4, we know that this simple adaptive two-grid method is also efficient for the L-shaped domain. Due to the singularity of the solution and the refinement strategy we use, the rate is not close to the second order. Here for adaptive grids, the second order h^2 is replaced by N^{-1}, where N is the number of unknowns. We would expect an optimal rate of convergence with more sophisticated adaptive edge finite element methods, e.g., [49].

Example 5.3

Consider the Maxwell eigenvalue problem on a three-dimensional domain $\Omega = (0, 1)^3$, $\mu_r = \varepsilon_r = 1$ in Ω. According to [17], we have $\lambda_1 = \lambda_2 = \lambda_3 = 2\pi^2$. We use the first family linear edge finite element to approximate $\boldsymbol{H}_0(\text{curl}; \Omega)$. In the same way as before, we retain the size of the coarse grid and of the fine mesh satisfying $H = h^3$, and the convergence rate of the two-grid scheme is nearly $\mathcal{O}(h^2)+\mathcal{O}(H^6)$. Table 5 supports our error estimate.

Example 5.4

Consider the Maxwell eigenvalue problem on a three-dimensional domain Ω, where Ω is a closed metallic cavity with a ridge along one of its faces. The coefficients $\mu_r = 1$ and $\varepsilon_r = 1$ in Ω. We consider a practical problem from engineering [12]. This domain is a rectangular cavity, air-filled, and has a metallic cavity with dimensions $1 \times 0.5 \times 0.75$ cm. For more information about the domain, see Figure 2 in [12]. A mesh of Ω is shown in our Figure 2. We do not know the exact solution to this problem; however, we did compare our results to those reported in [12]. Generally speaking, the smaller the mesh size, the better the accuracy. In this test, the two smallest eigenvalues are computed in the fine mesh, which has about 1 million unknowns. In Table 6, data1 and data2 come from [12]. We compared our results to those in [12], and found that our results are compatible with the results reported in [12]. The number of calls of the HX preconditioner is also stable to the mesh size but depends on the eigenvalue. As shown in [37], the major component of our algorithm, i.e., the HX preconditioner, is highly scalable. Based on the parallel implementation in the hypre library,[1] the HX preconditioner works nicely for a problem of size 78 million on 1024 processors. Therefore, we expect that our two-grid algorithms, which are mainly based on the HX preconditioner, will be effective and efficient for large-scale Maxwell eigenvalue problems based on similar parallel implementation.

6. Conclusion

In this paper, we have proposed two two-grid methods for the Maxwell eigenvalue problem. These methods only need to solve a general eigenvalue problem on the coarse grid and then solve one linear equation on the fine mesh using an efficient iterative method. We also have shown the asymptotic error estimate of the two-grid methods. Finally, we have presented several numerical experiments including two- and three-dimensional cases in order to confirm our theories.

[1] hypre: high-performance preconditioner, http://www.llnl.gov/CASC/hypre/.

Acknowledgments

We would like to thank the reviewers for their helpful comments and suggestions, especially for pointing out a gap in the original convergence proof of multiple eigenvalues.

The first author was supported by 2012–2013 China Scholarship Council (CSC) and Graduate Innovation Program of Hunan Province in China (CX2012B240). The fourth author was supported by the Program for Changjiang Scholars and Innovative Research Team in University of China (IRT1179), the Specialized Research Fund for the Doctoral Program of Higher Education (20124301110003), and the Scientific Research Fund of Hunan Provincial Education Department (12A138).

This author supported China was by Scholarship Council (201306755001), the National Natural Science Foundation of China under grant 11201159, the Foundation for the Author of National Excellent Doctoral Dissertation of PR China under grant 201212, the Zhujiang Technology New-Star Foundation of Guangzhou under grant 2013J2200063, and the Foundation for Outstanding Young Teachers in Higher Education of Guangdong Province under grant Yq2013054.

This author was supported by NSF grant DMS-1115961 and in part by Department of Energy prime award DE-SC0006903 and NIH grants P50GM76516.

References

1. Arbenz P, Geus R. Multilevel preconditioned iterative eigensolvers for Maxwell eigenvalue problems. Appl Numer Math. 2005; 54:107–121.
2. Arbenz P, Geus R, Adam S. Solving Maxwell eigenvalue problems for accelerating cavities. Phys Rev Accelerators and Beams. 2001; 4:022001.
3. Arnold DN, Falk RS, Winther R. Multigrid in H (div) and H (curl). Numer Math. 2000; 85:197–217.
4. Babuška I, Osborn J. Finite element-Galerkin approximation of the eigenvalues and eigenvectors of selfadjoint problems. Math Comp. 1989; 52:275–297.
5. Bank RE. Analysis of a multilevel inverse iteration procedure for eigenvalue Anal. problems. J Numer. 1982; 19:886–898.
6. Boffi D. Fortin operator and discrete compactness for edge elements. Numer Math. 2000; 87:229–246.
7. Boffi D. Finite element approximation of eigenvalue problems. Acta Numer. 2010; 19:1–120.
8. Boffi D, Fernandes P, Gastaldi L, Perugia I. Computational models of electromagnetic resonantors: Analysis of edge element approximation. SIAM J Numer Anal. 1999; 36:1264–1290.
9. Buffa A, Ciarlet P, Jamelot E. Solving electromagnetic eigenvalue problems in polyhedral domains with nodal finite elements. Numer Math. 2009; 113:497–518.
10. Buffa A, Houston P, Perugia I. Discontinuous Galerkin computation of the Maxwell eigenvalues on simplicial meshes. J Comput Appl Math. 2007; 204:317–333.
11. Caorsi S, Fernandes P, Raffetto M. On the convergence of Galerkin finite element approximations of electromagnetic eigenproblems. SIAM J Numer Anal. 2000; 38:580–607.
12. Chatterjee A, Jin JM, Volakis JL. Computation of cavity resonances using edge-based finite elements. IEEE Trans Microwave Theory Tech. 1992; 40:2106–2108.
13. Chen J, Xu Y, Zou J. An adaptive inverse iteration for Maxwell eigenvalue problem based on edge elements. J Comput Phys. 2010; 229:2649–2658.
14. Chen J, Xu Y, Zou J. An adaptive edge element method and its convergence for a saddle-point problem from magnetostatics. Numer Methods Partial Differential Equations. 2012; 228:1643–1666.
15. Chen Z, Wang L, Zheng W. An adaptive multilevel method for time-harmonic Maxwell equations with singularities. SIAM J Sci Comput. 2007; 29:118–138.
16. Chen, L. Technical report. University of California at Irvine; 2009. iFEM: An Integrated Finite Element Methods Package in MATLAB.
17. Ciarlet P Jr, Hechme G. Computing electromagnetic eigenmodes with continuous Galerkin approximations. Comput Methods Appl Mech Engrg. 2008; 198:358–365.

18. Dawson CN, Wheeler MF. Two-grid methods for mixed finite element approximations of nonlinear parabolic equations. Contemp Math. 1994; 180:191–191.
19. Dawson CN, Wheeler MF. A two-grid finite difference scheme for nonlinear parabolic equations. SIAM J Numer Anal. 1998; 35:435–452.
20. Dello Russo A, Alonso A. Finite element approximation of Maxwell eigenproblems on curved Lipschitz polyhedral domains. Appl Numer Math. 2009; 59:1796–1822.
21. Deuflhard, P.; Friese, T.; Schmidt, F. Technical report. Berlin: 1997. A Nonlinear Multigrid Eigenproblem Solver for the Complex Helmholtz Equation.
22. Erlangga Y. Advances in iterative methods and preconditioners Comput. for the Helmholtz equation. Arch Methods Engrg. 2008; 15:37–66.
23. Erlangga Y, Oosterlee C, Vuik C. A novel multigrid based preconditioner for heterogeneous Helmholtz problems. SIAM J Sci Comput. 2006; 27:1471–1492.
24. Girault V. Incompressible finite element methods for Navier-Stokes equations with nonstandard boundary conditions in R^3. Math Comp. 1988; 51:55–74.
25. Girault V, Lions JL. Two-grid finite-element schemes for the steady Navier-Stokes problem in polyhedra. Port Math. 2001; 58:25–58.
26. Girault, V.; Raviart, PA. Finite Element Methods for Navier–Stokes Equations: Theory and Algorithms. Springer-Verlag; Berlin: 1986.
27. Golub, GH.; Van Loan, CF. Matrix Computations. Johns Hopkins University Press; Baltimore, MD: 1996.
28. Hackbusch W. On the computation of approximate eigenvalues and eigenfunctions of elliptic operators by means of a multi-grid method. SIAM J Numer Anal. 1979; 16:201–215.
29. Hackbusch, W. Multi-Grid Methods and Applications. Springer-Verlag; Berlin: 1985.
30. Hiptmair R, Neymeyr K. Multilevel method for mixed eigenproblems. SIAM J Sci Comput. 2002; 23:2141–2164.
31. Hiptmair R. Finite elements in computational electromagnetism. Acta Numer. 2002; 11:237–339.
32. Hiptmair R, Xu J. Nodal auxiliary space preconditioning in H(curl) SIAM Numer. and H(div) spaces. J Anal. 2007; 45:2483–2509.
33. Hoyt HC. Numerical studies of the shapes of drift tubes and Linac cavities. IEEE Trans Nuclear Sci. 1965; 12:153–155.
34. Hu X, Cheng X. Acceleration of a two-grid method for eigenvalue problems. Math Comp. 2011; 80:1287–1301.
35. Kaya S, Riviere B. A two-grid stabilization method for solving the steady-state Navier-Stokes equations, Numer. Methods Partial Differential Equations. 2006; 22:728–743.
36. Kikuchi, F. Weak formulations for finite element analysis of an electromagnetic eigenvalue problem. Vol. 38. University of Tokyo; 1988. p. 43-67.Scientific Papers of the College of Arts and Sciences
37. Kolev T, Vassilevski PS. Parallel auxiliary space AMG for H(curl) problems. J Comput Math. 2009; 27:604–623.
38. Mandel J, McCormick S. A multilevel variational method for A u= λ B u on composite grids. J Comput Phys. 1989; 80:442–452.
39. Ilic M, Notaros B. Computation of 3-D electromagnetic cavity resonances using hexahedral vector finite elements with hierarchical polynomial basis functions. IEEE Trans Antennas Propagation. 2002; 4:682–685.
40. Monk, P. Finite Element Methods for Maxwell's Equations. Oxford University Press; Oxford, UK: 2003.
41. Parlett, B. The Symmetric Eigenvalue Problem. Classics in Appl. Math., SIAM; Philadelphia: 1998.
42. Peters G, Wilkinson J. Inverse iteration, ill-conditioned equations and Newton's method. SIAM Rev. 1979; 21:339–360.
43. Xu J. A new class of iterative methods for nonselfadjoint or indefinite problems. SIAM J Numer Anal. 1992; 29:303–319.

44. Xu J. A novel two-grid method for semilinear elliptic equations. SIAM J Sci Comput. 1994; 15:231–237.
45. Xu J. Two-grid discretization techniques for linear and nonlinear PDEs. J Numer Anal. 1996; 33:1759–1777.
46. Xu J, Zhou A. A two-grid discretization scheme for eigenvalue problems. Math Comp. 2001; 70:17–25.
47. Yang Y, Bi H. Two-grid finite element discretization schemes based on shifted-inverse power method for elliptic eigenvalue problems. SIAM J Numer Anal. 2011; 49:1602–1624.
48. Zaglmayr, S. Ph.D. thesis. Johannes Kepler University; Linz, Austria: 2006. High Order Finite Element Methods for Electromagnetic Field Computation.
49. Zhong L, Chen L, Shu S, Wittum G, Xu J. Convergence and optimality of adaptive edge finite element methods for time-harmonic Maxwell equations. Math Comp. 2012; 81:623–642.
50. Zhong L, Liu C, Shu S. Two-level additive preconditioners for edge element discretizations of time-harmonic Maxwell equations. Comput Math Appl. 2013; 66:432–440.
51. Zhong L, Shu S, Wang J, Xu J. Two-grid methods for time-harmonic Maxwell equations. Numer Linear Algebra Appl. 2013; 20:93–111.
52. Zhong L, Shu S, Wittum G, Xu J. Optimal error estimates for Nédélec edge elements for time-harmonic Maxwells equations. J Comput Math. 2009; 27:563–572.

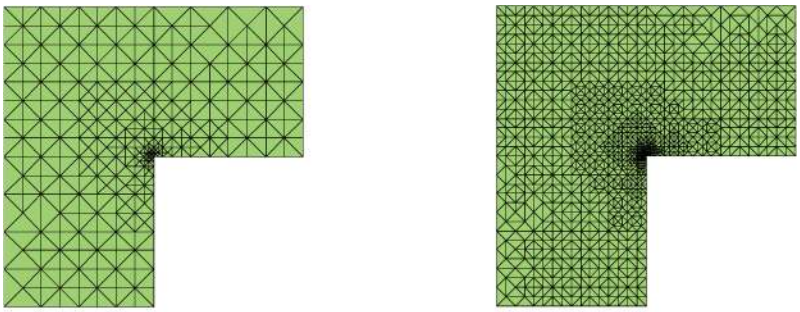

(a) Adaptive coarse mesh $\mathcal{T}_0$ (b) Adaptive fine mesh $\mathcal{T}_1$

Fig. 1.
Coarse and fine meshes with the adaptive method.

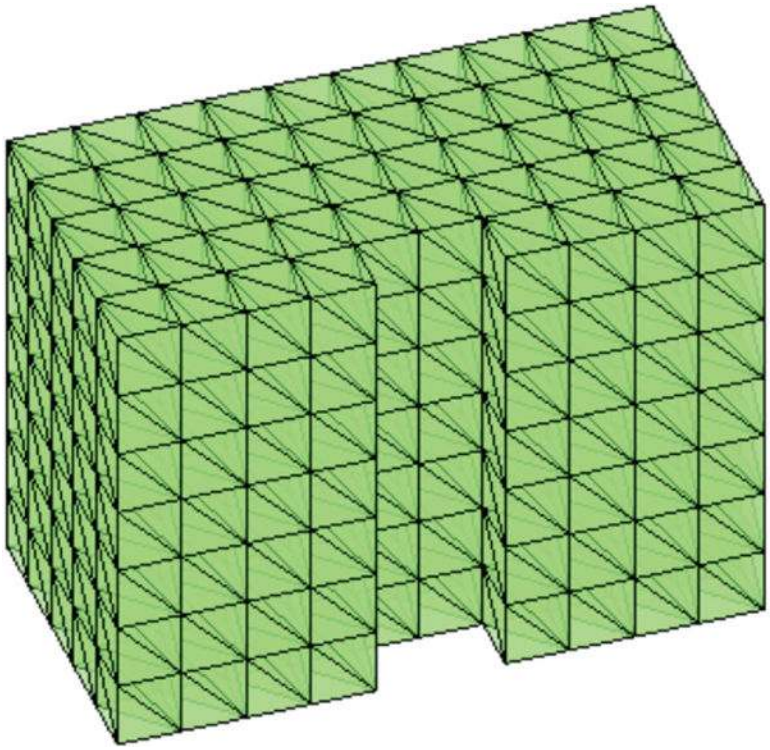

Fig. 2.
A coarse mesh used for Example 5.4.

Table 1

Fixed coarse mesh and varied fine meshes for Example 5.1.

k	H	h	$\lambda_{k,H}$	$\lambda_{k,h}$	λ_k^h	$\lambda_k - \lambda_k^h$	Rate	HX
1	1/16	1/32	9.867576	9.864823	9.869102	5.018558e-4		22
1	1/16	1/64	9.867576	9.868408	9.869479	1.251880e-4	2.00	28
1	1/16	1/128	9.867576	9.869305	9.869577	3.125953e-5	2.00	31
1	1/16	1/256	9.867576	9.869596	9.869597	7.458585e-6	2.04	30
2	1/16	1/32	9.867577	9.869102	9.869102	5.018558e-4		22
2	1/16	1/64	9.867577	9.869479	9.869479	1.251880e-4	2.00	28
2	1/16	1/128	9.867577	9.869573	9.869573	3.125953e-5	2.00	31
2	1/16	1/256	9.867577	9.869529	9.869597	7.458585e-6	2.04	30
3	1/16	1/32	19.760143	19.744481	19.744481	−5.272248e-3		29
3	1/16	1/64	19.760143	19.740529	19.740529	−1.320017e-3	2.00	33
3	1/16	1/128	19.760143	19.739539	19.739539	−3.316043e-4	2.00	33
3	1/16	1/256	19.760143	19.739291	19.739291	−8.993149e-5	1.92	30

Table 2

Fixed fine mesh and varied coarse meshes for Example 5.1.

k	H	h	$\lambda_{k,H}$	$\lambda_{k,h}$	λ_k^h	$\lambda_k - \lambda_k^h$	HX
1	1/8	1/512	9.793819	–	9.869578	2.711102e-5	33
1	1/16	1/512	9.850516	–	9.869585	1.965012e-5	35
1	1/32	1/512	9.864823	–	9.869585	1.953446e-5	30
1	1/64	1/512	9.868409	–	9.869585	1.953290e-5	31
2	1/8	1/512	9.861185	–	9.869602	2.892238e-6	33
2	1/16	1/512	9.867577	–	9.869602	2.800121e-6	35
2	1/32	1/512	9.869102	–	9.869602	2.798738e-6	30
2	1/64	1/512	9.869479	–	9.869602	2.798764e-6	31
3	1/8	1/512	19.820475	–	19.739226	−1.745514e-5	39
3	1/16	1/512	19.760143	–	19.739229	−1.997811e-5	38
3	1/32	1/512	19.744481	–	19.739229	−1.895603e-5	37
3	1/64	1/512	19.740529	–	19.739229	−1.895792e-5	33

Table 3

Varied coarse and fine meshes for Example 5.1 ($H^3 = h$).

k	H	h	$\lambda_{k,H}$	$\lambda_{k,h}$	λ_k^h	$\lambda_k - \lambda_k^h$	Rate	HX
1	1/2	1/8	8.808164	9.793819	9.770782	9.882168e-2		20
1	1/4	1/64	9.575132	9.868409	9.867936	1.667576e-3	5.89	29
1	1/8	1/512	9.793818	–	9.869578	2.711102e-5	5.94	33
2	1/2	1/8	9.600000	9.861185	9.859485	1.011926e-2		20
2	1/4	1/64	9.830558	9.869479	9.869471	1.335355e-4	6.23	29
2	1/8	1/512	9.861185	–	9.869602	2.892238e-6	5.52	33
3	1/2	1/8	20.287187	19.820475	19.818958	−7.975001e-2		26
3	1/4	1/64	20.023547	19.740529	19.740337	−1.128590e-3	6.14	35
3	1/8	1/512	19.820475	–	19.739229	−1.643085e-5	6.10	39

Table 4

Adaptive two-grid for L shape domain problem.

H	Dof (H)	h	Dof (h)	λ_1	$\lambda_1 - \lambda_1^h$	Rate
$\mathscr{T}_0$	834	$\mathscr{T}_1$	4268	1.473409	2.0131e-3	-
$\mathscr{T}_0$	834	$\mathscr{T}_2$	12984	1.475034	5.8748e-4	1.78
$\mathscr{T}_0$	834	$\mathscr{T}_3$	51696	1.475444	1.7778e-4	1.72

Table 5

Varied coarse and fine mesh for Example 5.3 ($H^3 = h$).

k	*H*	*h*	λ_k^h	$\lambda_k - \lambda_k^h$	Rate	HX	Dof(h)
1	1/2	1/8	19.467320	2.718887e-1		24	4,184
1	1/4	1/64	19.734459	4.750711e-3	5.84	23	1,872,064
2	1/2	1/8	19.693282	4.592657e-2		17	4,184
2	1/4	1/64	19.738345	8.642775e-4	5.73	23	1,872,064
3	1/2	1/8	19.693283	4.592657e-2		17	4,184
3	1/4	1/64	19.738345	8.642775e-4	5.73	23	1,872,064

SIAM J Numer Anal. Author manuscript; available in PMC 2015 July 16.

Table 6

Two-grid results for Example 5.4 using the lowest order edge element.

N0	data1	data2	Coarse	Fine 1	HX	Fine 2	HX	Fine 3	HX
Dof	267	671	2855	20,782		158,300		1,235,128	
1	4.941	4.999	5.051	5.077	24	5.087	23	5.091	26
2	7.284	7.354	7.394	7.446	45	7.462	47	7.468	49